

LROC WAC ULTRAVIOLET REFLECTANCE OF THE MOON. M. S. Robinson¹, B. W. Denevi², H. Sato¹, B. Hapke³, B. R. Hawke⁴, ¹School of Earth and Space Exploration, Arizona State University, Tempe AZ, ² Johns Hopkins University Applied Physics Laboratory, Laurel MD, ³University Pittsburgh, Pittsburgh PA, ⁴SOEST, Univ. HI, Honolulu HI.

Introduction: Pioneering color filter photography first showed color differences related to morphologic boundaries on the Moon [1]. These color units were interpreted to indicate compositional differences, thought to be the result of variations in titanium content [1]. Later it was shown that iron abundance (FeO) also plays a dominant role in controlling color in lunar soils [2]. Equally important is the maturity of a lunar soil in terms of its reflectance properties (albedo and color) [3]. Maturity is a measure of the state of alteration of surface materials due to sputtering and high velocity micrometeorite impacts over time [3].

The Clementine (CL) spacecraft provided the first global digital visible through infrared observations of the Moon [4]. This pioneering dataset allowed significant advances in our understanding of compositional (FeO and TiO₂) and maturation differences across the Moon [5,6]. Later, the Lunar Prospector (LP) gamma ray and neutron experiments provided the first global, albeit low resolution, elemental maps [7]. Newly acquired Moon Mineralogic Mapper hyperspectral measurements are now providing the means to better characterize mineralogic variations on a global scale [8].

Our knowledge of ultraviolet color differences between geologic units is limited to low resolution (km scale) nearside telescopic observations, high resolution Hubble Space Telescope images of three small areas [9], and laboratory analyses of lunar materials [10,11]. These previous studies detailed color differences in the UV (100 to 400 nm) related to composition and physical state. HST UV (250 nm) and visible (502 nm) color differences were found to correlate with TiO₂, and were relatively insensitive to maturity effects seen in visible ratios (CL) [9]. These two results led to the conclusion that improvements in TiO₂ estimation accuracy over existing methods may be possible through a simple UV/visible ratio [9].

The Lunar Reconnaissance Orbiter Camera (LROC) Wide Angle Camera (WAC) provides the first global lunar ultraviolet through visible (321 nm to 689 nm) multispectral observations [12]. The WAC is a seven-color push-frame imager with nominal resolutions of 400 m (321, 360 nm) and 100 m (415, 566, 604, 643, 689 nm). Due to its wide field-of-view (60° in color mode) the phase angle within a single line varies ±30°, thus requiring the derivation of a precise photometric characterization [13] before any interpretations of lunar reflectance properties can be made. The current WAC photometric correction relies on

multiple WAC observations of the same area over a broad range of phase angles and typically results in relative corrections good to a few percent [13].

WAC Color Observations: A global 7-band mosaic was constructed from photometrically corrected images collected over one month, and sampled to 400 m/pixel. Three band color reconstructions and color ratio images were inspected to guide selection of spectral areas that represent the range of color differences within the dataset. Extracted spectra were normalized to a highlands area (34.71°S, 39.80°E) to minimize remaining absolute calibration inaccuracies (Fig. 1). Units were divided based on spectral slope in UV (321 to 415 nm) and visible (415 to 689 nm). Units with positive UV slope (UV color index) are labeled +UCI, and those with negative UV color index -UCI. Likewise, units with positive visible slope (visible color index) are labeled +VCI, and those with negative visible color index -VCI.

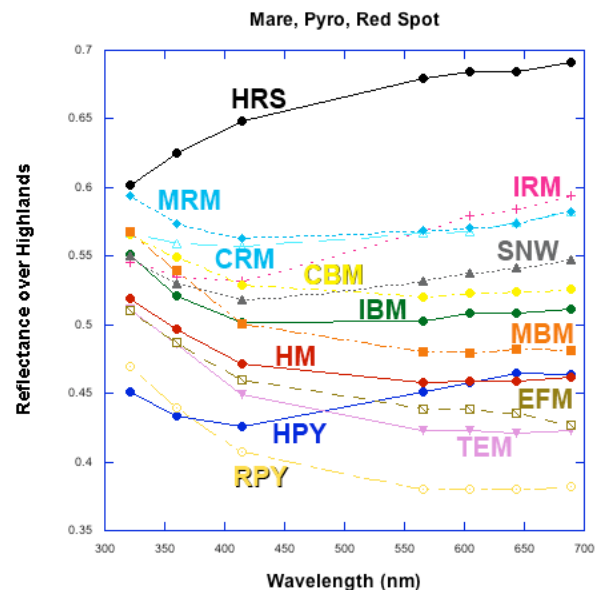


Fig. 1. Normalized WAC spectra for range of lunar materials. HRS Helmet red spot, MRM Moscoviense red mare, IRM Imbrium red mare, CRM Cognitum red mare, SNW Serenitatis NW mare, CBM Cognitum blue mare, IBM Imbrium blue mare, MBM Moscoviense blue mare, HM Humorum mare, EFM east Fecunditatis mare, HPY Humorum pyroclastics, TEM Tranquillitatis east mare, RPY Rima Bode pyroclastic. Red and blue follow convention for visible observations of mare.

Maturity. Very young Copernican materials (*i.e.* Giordano Bruno, Tycho craters) have +UCI and -VCI.

For middle to early Copernican materials the UCI is slightly positive to flat indicating that lunar materials mature relatively fast at UV wavelengths [9,14]

Red spots. Anomalously red regions known as red spots, and often associated with domes [15], exhibit +UCI and +VCI and their normalized spectra (HRS, Fig. 1) typically flatten out past 566 nm. A tongue of ejecta on the SE rim of Aristarchus crater exhibits spectral properties akin to red spots and may represent excavated intrusive red spot material.

Pyroclastic deposits. Pyroclastic deposits all show -UCI but their VCI ranges significantly from negative (RPY) through positive (HPY).

Mare. Mare units all exhibit a -UCI and a variable VCI (classic descriptions of red and blue mare). Mare units with steeper -UCI correlate with areas previously mapped as enriched in TiO₂.

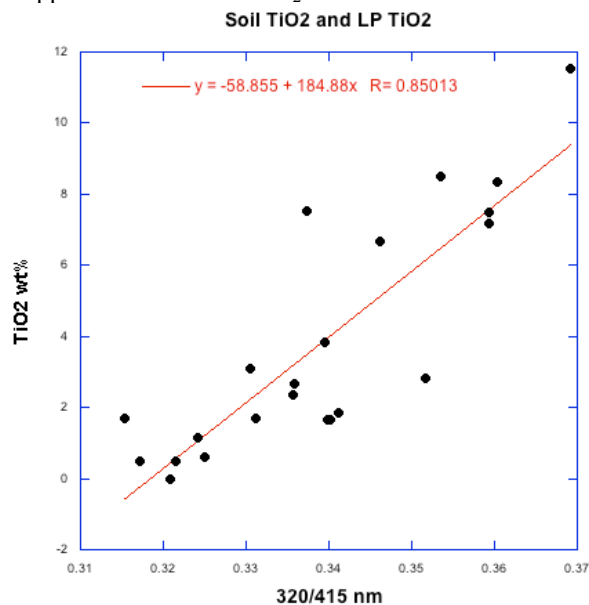


Fig 2. Lunar surface TiO₂ vs. WAC 320/415 nm.

Titanium mapping. To test the hypothesis of [9] that a simple UV to visible ratio follows TiO₂ abundance in lunar soils, we fitted LP [16] and sample TiO₂ values to WAC 321/415 nm ratio. Average soil TiO₂ values for Apollo and Luna sites are described in [5]. Luna 16 site was not used because its location in the WAC mosaic is on a calibration defect. Luna 24 was also excluded as it likely represents subsurface material ejected in an impact event. Obtaining LP TiO₂ values to match WAC ratios was more challenging due to the gross mismatch in resolutions between the two datasets (~50km and 400 m, respectively). The WAC mosaic was resampled to 10 km; small areas that were relatively invariant in the 10-km WAC data were selected as tie points to the LP map. The combined soil

sample and LP TiO₂ values were fitted to the corresponding WAC 321/415 nm ratio values ($n=21$) with an r -value of 0.85 (Fig. 2). The goodness of fit indicates that the 321/415 nm ratio is dominantly controlled by TiO₂ abundance as hypothesized by [9]. A global WAC 321/415 nm ratio map was inverted to TiO₂ (Fig. 3). The highest values in the WAC TiO₂ map are in eastern mare Tranquillitatis (average 9 wt%, maximum 11 wt%) and the highlands are generally less than 0.5 wt%. Red spots have large negative TiO₂ values (<-3 wt%) and thus do not follow the mapping trend. We are currently evaluating the efficacy of the method for mapping TiO₂ in pyroclastic deposits (e.g. Aristarchus 1 wt%, Rima Bode 9 wt%).

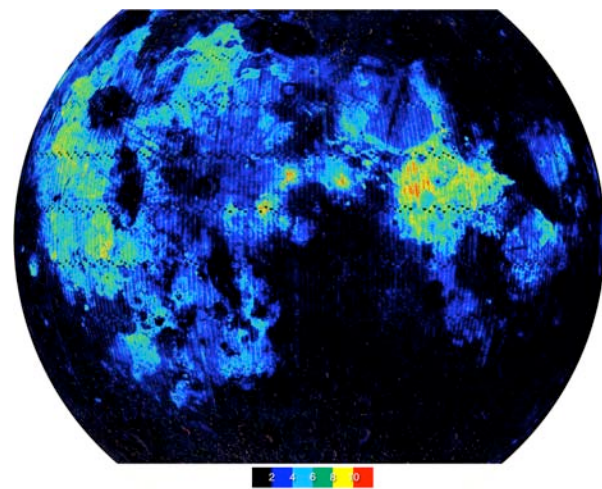


Fig. 3. LROC WAC TiO₂ map of lunar nearside, vertical artifacts are remaining are due to remaining uncertainties in the photometric correction [13].

References: [1] Whitaker E. A., *The Moon*, 4, 348-355, 1972. [2] Adams J. B. et al., (1981) *Basaltic Volcanism on the Terrestrial Planets*, 439-490, Pergamon, NY. [3] Hapke B. (2001), *JGR*, 106, 10,039– 10,073. [4] Nozette S. et al (1994) *Science*, 266, 1835–1839. [5] Blewett D. T. et al. (1997) *JGR*, 102, 16,319–16,325. [6] Lucey P. G. et al. (2000) *JGR*, 105, 20,297–20,305. [7] Feldman W.C. et al. (2002), *JGR*, 107, 10.1029/ 2001JE001506. [8] Green R.O. (2008) *LPSC XXXIX*, 1803. [9] Robinson et al. (2007) *GRL*, 34, 10.1029/ 2007GL029754 [10] Hapke B. et al. (1978) *PLPSC 9th*, 2935-2947. [11] Wagner J.K. et al. (1987) *Icarus*, 69, 14-28. [12] Robinson M.S. et al. (2010) *Space Sci. Rev.*, 150, 81-124. [13] Sato H. et al., this volume. [14] Denevi B.W. et al., this volume. [15] Malin M.C. (1974) *Earth Planet. Sci. Lett.*, 21, 331-341. [16] Prettyman T.H. et al. (2006) *JGR*, 111, 1029/ 2005JE002656.